

Optical Properties and Raman Studies of Amorphous Se-Bi Thin Films

Austine A. Mulama^{1,*}, Julius M. Mwabora², Andrew O. Oduor¹ and Cosmas C. Muiva³

¹*Department of Physics and Materials Science, Maseno University, Maseno, Kenya*

²*Department of Physics, University of Nairobi, Nairobi, Kenya*

³*Department of Physics, Botswana International University of Science and Technology, Gaborone-Botswana*

Flash evaporated amorphous $\text{Se}_{100-x}\text{Bi}_x$ ($x = 0, 1, 2, 3$, and 4 at. %) thin films of $350 \pm 10\text{nm}$ thickness have been investigated in the wavelength range of $200\text{nm} - 3000\text{nm}$. It is found that the effect of increasing bismuth content on the as deposited films led to increased absorption coefficient, reflectance, refractive index and extinction coefficient while transmittance and optical band gap energy decreased. The Raman spectra showed peaks at 238.8cm^{-1} , 248.3cm^{-1} , 249.5cm^{-1} , 250.7cm^{-1} , 251.9cm^{-1} , 488.1cm^{-1} , and 489.3cm^{-1} due to selenium rings and chains at various bismuth concentrations.

1. Introduction

Chalcogenide glasses are composed of chalcogen elements (selenium, sulphur and tellurium) of group VI of the periodic table. There is an increased interest in the properties of amorphous selenium (a-Se) rich semiconducting alloys due to their current use as photoconductors in high definition television (TV) pick-up tubes and in digital X-ray imaging [1]. Chalcogenide glasses of a-Se are largely used in memory devices and fiber optics as they exhibit threshold and memory switching behavior as well as infrared transmission [2].

Pure a-Se is less sensitive to electromagnetic radiation. In addition, the glass transition temperature of a-Se is just above room temperature ($\sim 42^\circ\text{C}$), which makes a-Se rather unstable and in danger of unintended crystallization. To stabilize a-Se matrix, certain additives are added, in the order of about 1 at. %. These include lead (Pb), arsenide (As), bismuth (Bi), among others [3]. The glass transition temperature of stabilized a-Se is about 70°C [4]. The study focuses on the role of Bi in affecting the optical properties of a-Se films. Limited work is reported on the Raman studies of the as deposited Se-Bi thin films. Addition of bismuth to selenium films is said to increase the stability, sensitivity of the films and changes the conductivity from p-type to n-type [5]. It also serves to increase the chemical and thermal stability of the amorphous selenium glass. Hence, the role of bismuth addition to amorphous selenium is interesting.

2. Experimental Details

Glassy alloys of $\text{Se}_{100-x}\text{Bi}_x$ ($x = 0, 1, 2, 3$, and 4 at. %) were prepared by melt quenching technique. Selenium and bismuth of purity 99.999% were weighed according to their atomic percentages in powder form on the electronic balance (LIBROR, AEG-120; Japan). The weighed samples were sealed in quartz ampoules vacuumed to $5.0 \times 10^{-5}\text{mbar}$ (Edwards Auto 306 Vacuum System, UK). The sealed ampoules were kept in a rotatable programmable furnace where the temperature was raised to 690°C at a rate of 4°C per minute and maintained at this temperature for 12 hours, to get a complete melt and a homogeneous mixture. The ampoules were quenched in ice cold water at 690°C to form amorphous samples. The temperature of 690°C ensured that the molecules in the amorphous samples remained at a constant concentration [6]. The ampoules were broken to obtain the solid alloy that was crushed into powder for flash evaporation.

The material powder was placed inside a vibrating tube enclosed inside an evaporation chamber that was vacuumed to $3.0 \times 10^{-5}\text{mbar}$ (Edwards AUTO 306 Vacuum system, UK). The powder fell grain by grain to a preheated tungsten boat. The vapours were collected on cleaned glass substrates forming thin films. The optimum substrate-source distance was 10cm . The deposition rate was 25\AA s^{-1} . The melt quenching step, flash evaporation and low deposition rate helped achieve a film composition that was close to the bulk starting material [7].

The amorphous nature of the deposited films was verified by X-Ray Diffraction machine

*mulamaustine@gmail.com

(Phillips PW3710, UK). Film thickness of $350 \pm 10\text{nm}$ was determined using a computerized KLA-Tencor Alpha-Step IQ surface profiler (KLA-Tencor Corporation, USA). The surface profiler had a resolution of $0.01\mu\text{m}$. Transmittance and reflectance measurements were made using a SolidSpec.3700 DUV, Spectrophotometer (SolidSpec.3700 DUV, Kyoto-Japan). The optical transmission spectra in the wavelength range $200\text{nm}-3000\text{nm}$ have been used to calculate the optical parameters of the amorphous thin films of $\text{Se}_{100-x}\text{Bi}_x$.

The Raman Spectroscopy used was an STR Raman Spectrometer (SEKI Technotron Corporation, Tokyo-Japan).

3. Results

3.1. Transmittance and reflectance of $\text{Se}_{100-x}\text{Bi}_x$ thin films

For maximum transmission [8]

$$T = \exp - (\alpha d) \tag{1}$$

Where, α is the absorption coefficient and d is the film thickness

The transmission curves in Fig. 1 show that for lower wavelengths ($\leq 500\text{nm}$) corresponding to high energies, the transmittance is zero because most of the light is absorbed. This is the region of strong absorption and has very large absorption coefficient ($7.88 \times 10^4\text{cm}^{-1} \leq \alpha \leq 3.56 \times 10^5\text{cm}^{-1}$). The reflectance values increases as bismuth concentration increases from $x = 0$ to $x = 4 \text{ at. \%}$ at specific wavelengths due to the effect of transmission of light in the as deposited thin films (Fig. 1).

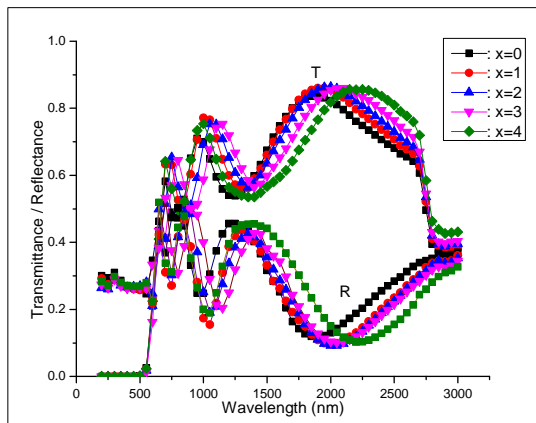


Fig.1: Transmittance and reflectance against wavelength (nm) for $\text{Se}_{100-x}\text{Bi}_x$ thin films.

Interference patterns can be observed from Fig. 1. This may be due to the interference between the wave fronts generated at the air and substrate interface, which defines the sinusoidal behavior of the curves.

3.2. Absorption coefficient and extinction coefficient of $\text{Se}_{100-x}\text{Bi}_x$ thin films

The optical absorption coefficient from Fig. 2 increases with an increase in photon energy and with increase in bismuth content. For low energies, corresponding to high wavelengths, thin film interference effects are observed from Fig. 2. This may be due to the overlaying of light that is reflected on both sides of the as deposited thin films of $\text{Se}_{100-x}\text{Bi}_x$.

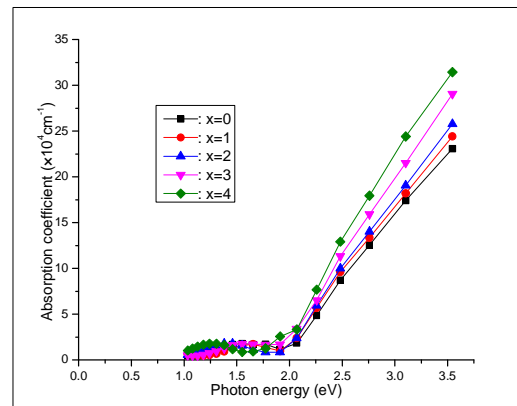


Fig.2: Absorption coefficient against photon energy (eV) for $\text{Se}_{100-x}\text{Bi}_x$ thin films.

The increase in extinction coefficient values with an increase in bismuth concentration from $x = 0$ to $x = 4 \text{ at. \%}$ have been observed from Fig. 3.

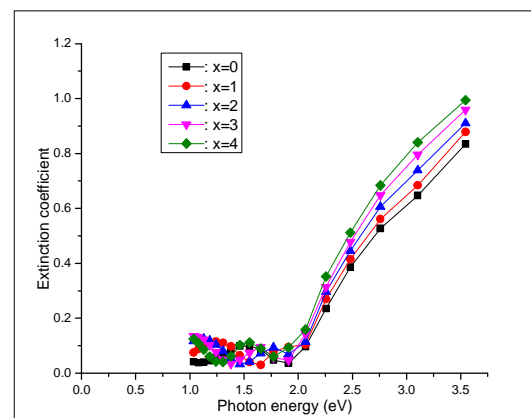


Fig.3: Extinction coefficient against photon energy (eV) for $\text{Se}_{100-x}\text{Bi}_x$ thin films.

The rise and fall of extinction coefficient in the forbidden gap region is directly related to the absorption of light.

3.3. Refractive index and real part of the dielectric constant of $Se_{100-x}Bi_x$ thin films

The method used to determine the refractive index in this study was the Swanepoel envelope method [9]. The first step was to calculate the maximum and minimum transmittance envelop functions, T_M and T_m , respectively. From these functions, n can be found

$$n = [N + (N^2 - s^2)^{1/2}]^{1/2} \tag{2}$$

Where

$$N = 2s \frac{T_M - T_m}{T_M T_m} + \frac{s^2 + 1}{2} \tag{3}$$

Here, s is the refractive index of the glass substrate ($s = 1.52$).

Real (ϵ_1) and imaginary (ϵ_2) parts of the dielectric constant are given by [8,9]

$$\epsilon_1 = n^2 - k^2 ; \epsilon_2 = 2nk \tag{4}$$

Fig. 4 shows that the refractive index decreases with the increase in the wavelength. In addition, the refractive index increases with an increase in the bismuth concentration from $x = 0$ to $x = 4$ at. % [10,11].

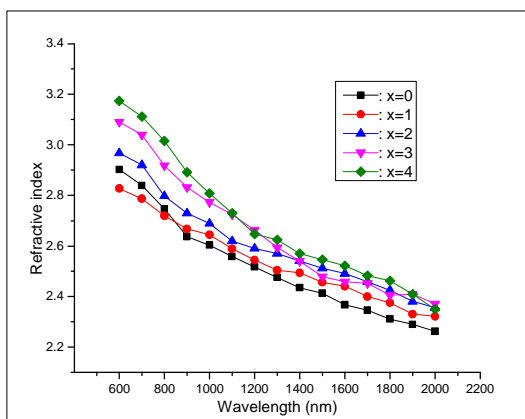


Fig.4: Refractive index against wavelength (nm) for $Se_{100-x}Bi_x$ thin films.

The real part of the dielectric constant against wavelength decreases with increase in wavelength, as shown in Fig. 5.

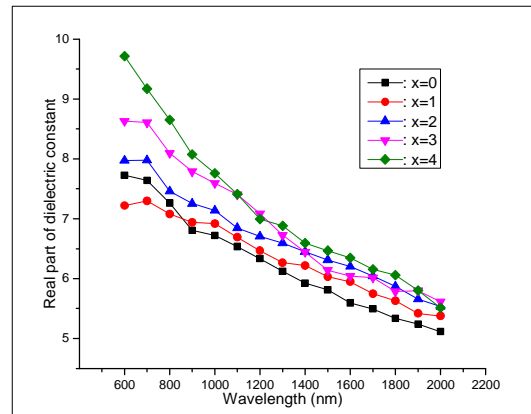


Fig.5: Real part of dielectric constant against wavelength (nm) for $Se_{100-x}Bi_x$ thin films.

3.4. Optical band gap energy of $Se_{100-x}Bi_x$ thin films

The plots of $(\alpha hv)^{1/2} (eVcm^{-1})^{1/2}$ against photon energy (eV) were used to get the optical band gap energy of the as deposited $Se_{100-x}Bi_x$ thin films. This was done by extrapolating the graph to the energy axis using Eqn. (5) for $m = 2$ according to Tauc proposal for most amorphous semiconductors [12].

$$\alpha hv = \xi (hv - E_g)^m \tag{5}$$

Where, α is the absorption coefficient, ξ is a constant, hv is the photon energy. The values of m represent the following transitions: for $m = 1/2$ a direct allowed transition, $m = 3/2$ for a direct forbidden transition, $m = 2$ for an indirect allowed transition, and $m = 3$ for an indirect forbidden transition [13].

The graphs in Fig. 6 are nonlinear, indicating that the transition in the forbidden gap is indirect and allowed. In a material free from any imperfections, only direct but allowed transition can take place from the valence to the conduction band. In the presence of defects, impurities, dislocations and other imperfections like the system under study, one has to consider the perturbation of the system due to their presence and also their interactions with phonons. All these give rise to the indirect and its other related transitions [14].

The optical band gap energy, as observed from Fig.7, decreased with the increase in bismuth content. Similar trend has been observed by other authors [11,13,15]. The band gap energy decreased from 1.38eV to 1.24eV for the $350 \pm 10nm$ thin films.

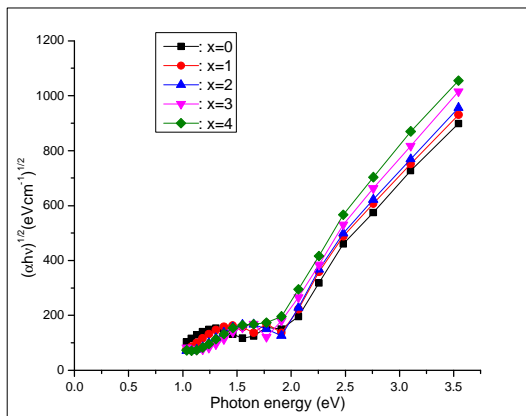


Fig.6: $(\alpha hv)^{1/2} (eV cm^{-1})^{1/2}$ against photon energy (eV) for $Se_{100-x}Bi_x$ thin films.

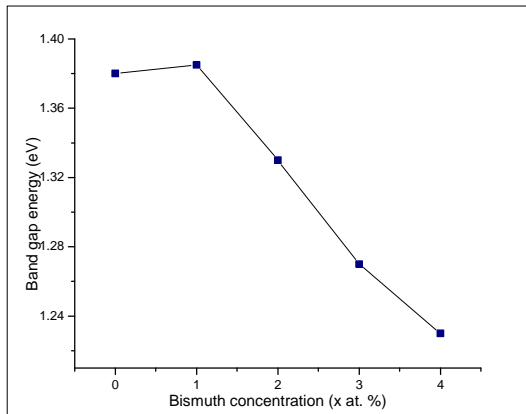


Fig.7: Band gap energy (eV) against bismuth concentration for $Se_{100-x}Bi_x$ thin films.

3.5. Raman spectra analysis of $Se_{100-x}Bi_x$ thin films

Selenium consists of a mixture of chains (Se_n) and rings (Se_8) with covalent bonding of the atoms in rings and Van der Waals weak bonding between the atoms in chains. Fig. 8 gives the plot of Raman intensity against wave numbers (cm^{-1}) for the films under study.

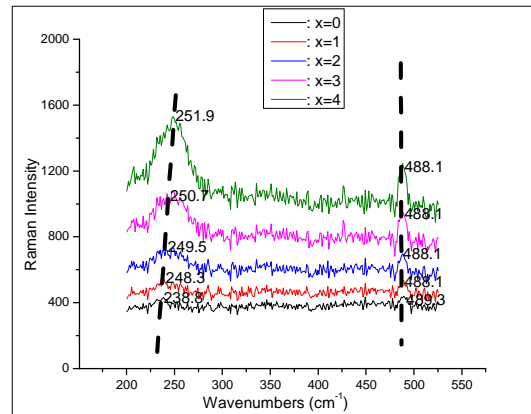


Fig.8: Raman spectra for $Se_{100-x}Bi_x$ thin films.

4. Discussions

The region between 500nm and 800nm has medium absorption and the transmission is ≤ 0.80 . This is because of the effect of the absorption coefficient in the range of $6.06 \times 10^3 cm^{-1} \leq \alpha \leq 14.11 \times 10^4 cm^{-1}$. In this region, most of the optical transitions take place between localized tail states and extended band states. In the transparent region ($\geq 900nm$), the absorption coefficient is low ($\alpha \leq 4.68 \times 10^2 cm^{-1}$). This is the region that is away from the electronic and vibrational resonances. It is the region of low energy absorption that originates from defects and impurities and in this case from bismuth content on the as deposited $Se_{100-x}Bi_x$ thin films. Here, the transmission is determined by the refractive index of the film and the refractive index of the substrate through multiple reflections [15]. As the concentration of bismuth increases from $x = 0 at. \%$ to $x = 4 at. \%$, the transmission of light in the as deposited $Se_{100-x}Bi_x$ thin films decreases. This is mainly due to the effect of bismuth introduced in the selenium films as impurity. As a result, the absorption coefficient increases.

The optical absorption coefficient, as shown in Fig. 2, increases with an increase in photon energy and with an increase in bismuth content. There is a relatively sharp delimitation between the areas of high and low absorption. This may be an indication of an increase in photosensitivity of the as deposited thin films with bismuth addition. This trend fits well with already published work [11].

An increase in the extinction coefficient values with an increase in the bismuth concentration from $x = 0$ to $x = 4 at. \%$ results from the increased absorption coefficient of the as deposited thin films with bismuth concentration. As bismuth is introduced to host selenium films, bismuth atom

addition is incorporated in the cross-linking the selenium chains by bonding with selenium atoms. Increase in refractive index as the bismuth content increases may be due to increased polarizability of the larger bismuth atoms compared to selenium atoms. The atomic radius of bismuth is 1.50\AA and that of selenium is 1.20\AA [16]. The high polarizability of the chalcogenide glasses causes them to exhibit the highest intrinsic nonlinear response.

Introduced bismuth atoms leads to the formation of the heteropolar Se-Bi bonds (bond energy 40.7kcalmol^{-1}) at the expense of the homopolar Se-Se bonds (bond energy 44.4kcalmol^{-1}) [2,17]. This leads to a decrease in the concentration of Se-Se bonds. Therefore, increasing the concentration of Bi atoms in the $Se_{100-x}Bi_x$ system could decrease the glass bond energies and consequently its optical energy gap. The number of Se-Bi bonds increase with an increase in bismuth concentration. In addition, bismuth is said to partly break the Se_8 ring structure (covalently bonded) and this may increase the chain fraction (Van der Waals bonded), that could lead to decreased optical energy gap of the system [17]. The decrease in the optical band gap energy may also be due to decrease in cohesive energy of the system, which is the stabilization energy of an infinitely large cluster of the material per atom determined by summing the bond energies of the consequent bonds expected in the as deposited films [18]. The expected bonds in this study are Se-Se and Se-Bi. The formation of Bi-Bi bonds is ruled out as it is argued that their bond energy is lower than that of the Se chains [19]. The average cohesive energy of all the bonds expected in the as deposited thin films of $Se_{100-x}Bi_x$ is therefore low, leading to reduced optical band gap energy. This is because the optical band gap energy is sensitive to bond energy [20]. From Fig. 7, we note that the band gap energy of the as deposited thin films of $Se_{100-x}Bi_x$ ($x = 0, 1, 2, 3$ and 4 at. %) increases slightly at $x = 1$ at. % and then decreases with an increase in the bismuth concentration. The increase may be due to shift in Fermi level and the decrease may be due to increase in density of defect states in the as deposited thin films [21]. This result is in agreement with already published work [11].

For pure amorphous selenium film, $x = 0$ at. %, the Raman spectrum has been characterized by a strong band at 238.8cm^{-1} and this could be attributed to the vibrational mode of $-Se - Se - Se -$ chains that occurs at a value near

or equal to 238cm^{-1} [22]. The obtained value is in agreement with already published work. For instance, 237cm^{-1} [23], 239cm^{-1} [24], have been found. Our Raman peak is close to Adam's value [24]. As the bismuth concentration increases, the 238.8cm^{-1} peak disappears. This is attributed to the contraction of inter-atomic bonds resulting in breaking Se chains by the bismuth addition, making favourable conditions for ring molecule formation. The Raman bands increase in intensity up to 251.9cm^{-1} , a value that is in agreement with the expected peak for a selenium rich binary glass whose peak is usually in the range $247\text{cm}^{-1} - 260\text{cm}^{-1}$ [25,26]. The obtained peak values fit well with already published work for selenium binary glass alloy like 252cm^{-1} [25], 250cm^{-1} , 248.5cm^{-1} , 247.5cm^{-1} [26]. The peaks at 489.3cm^{-1} and 488.1cm^{-1} could be associated with selenium ring due to a two-phonon resonance of Se_8 ring molecule according to *Siemsen* and *Riccus*, who assigned the peak at 490cm^{-1} to a two-phonon resonance of Se_8 ring molecule [27]. The peaks are less than 490cm^{-1} and this could be as a result of bismuth defects in the deposited films.

5. Conclusions

The transmission of light in the as deposited thin films decreased at specific wavelengths with an increase in the bismuth concentration while the reflectance increased. The absorption coefficient increased with an increase in the bismuth concentration. The as deposited films seem to be more sensitive to light as the bismuth concentration increases as observed from the shift in transmittance graph towards the visible region. The extinction coefficient of the as deposited films increased with the increase both in photon energy and bismuth concentration. This was as a result of an increased absorption coefficient of the as deposited thin films.

The refractive index of the as deposited thin films obtained using the Swanepoel method decreased with the increase in wavelength, but increased with an increase in the bismuth concentration. The increase in refractive index was mainly due to the change in the mean polarizability of the system. The optical band gap energy decreased with an increase in the bismuth content. This has been explained in terms of decreased cohesive energy. The Raman spectra showed peaks at 238.86cm^{-1} , 248.3cm^{-1} , 249.5cm^{-1} , 250.7cm^{-1} , 251.9cm^{-1} , 488.1cm^{-1} , and 489.3cm^{-1} for the $Se_{100-x}Bi_x$ thin films.

Acknowledgments

The authors wish to thank the National Council for Science and Technology (Now Commission for Science, Technology and Innovation (NACOSTI)) for the 2012-2013 Science, Technology and Innovation (ST & I) 010545 grant support.

Mr. B. Muthoka and Mr. D. Omucheni are thanked for their help in experimental set ups and their valuable technical advice (University of Nairobi).

References

- [1] C. M. Muiva, T. S. Sathiaraj and J. M. Mwabora, *The Eu. Phys. J. Appl. Phys.* **59**, 1 (2012).
- [2] A. H. Moharram, *Thin Solid Films* **392**, 1, 34 (2001).
- [3] E. A. Davis, *Electronic and Structural Properties of Amorphous Semiconductors*, Eds. P. G. I. Lecomber and J. Mort (Academic Press, N. Y., London, 1973)
- [4] N. Kushwaha, V. S. Kushwaha, R. K. Shukla and A. Kumar, *J. Non-Cryst. Solids* **351**, 3414- (2005).
- [5] S. R. Elliot and A. T. Steel, *J. Phys. C: Solid State Phys.* **20**, 4335 (1987).
- [6] A. S. Soltan, M. Abu El-Oyoun, A. A. Abu-Sehly and A. Y. Abdel-Latif, *Mat. Chem. Phys.* **82**, 101 (2003).
- [7] E. Marquez, A. M. Bernal-Oliva, J. M. Gonzalez-Leal, R. Prieto-Alcon, A. Ledesma, R. Jimenez-Garay and I. Martil, *Mat. Chem. Phys.* **60**, 3, 231 (1999).
- [8] M. Born and E. Wolf, *Principles of Optics*, seventh edition (Cambridge University Press, London, 1999).
- [9] R. Swanepoel, *J. Phys. E: Sci. Instrum.* **16**, 1214 (1983).
- [10] P. Sharma, I. Sharma and S. C. Katyal, *J. Appl. Phys.* **105**, 053509, 1 (2009).
- [11] M. A. Majeed Khan, M. Zulfequar and M. Husain, *Opt. Mat.* **22**, 21 (2003).
- [14] J. Tauc, *Amorphous and Liquid Semiconductors* (Plenum Press, London, 1974).
- [15] K. Kumar, P. Sharma, S. C. Katyal and N. Thakur, *Phys. Scr.* **84**, 045703, 1 (2011).
- [16] A. Kumar, P. Heera, P. B. Barman and R. Sharma, *J. Ovonic Res.* **8**, 5, 135 (2012).
- [17] J. Schottmiller, M. Tabak, G. Lucovsky and A. Ward, *J. Non-Cryst. Solids* **4**, 80 (1970).
- [18] K. Kumar, N. Thakur, S. C. Katyal and P. Sharma, *Defect and Diffusion Forum*, **305/306**, 61 (2010).
- [19] M. M. Hafiz, A. A. Othmana, M. M. El-Nahassb and A. T. Al-Motasema, *Physica B* **390**, 348 (2007).
- [20] J. Bicerano and S. R. Ovshinsky, *J. Non-Cryst. Solids* **74**, 1, 75 (1985).
- [21] N. F. Mott and E. A. Davis, *Electronic Processes in Non-Crystalline Materials*, second edition (Clarendon Press, Oxford, 1979).
- [22] V. Kovanda, Mir. Vicek and H. Jain, *J. Non-Cryst. Solids* **326 & 327**, 88 (2003).
- [23] J. Wieszka, Ph. Daniel, A. M. Burian, A. Burian and M. Zelechower, *Solid State Comm.* **119**, 533 (2001).
- [24] A. B. Adam, *New Horizons in Science and its Applications*, 1-6 (2007).
- [25] M. S. Iovu, E. I. Kamitsos, C. P. E. Varsamis, P. Boolchand and M. Popescu, *Chalcogenide Letters*, **2**, 3, 21 (2005).
- [26] R. Lukács, M. Veres, K. Shimakawa and S. Kugler, *J. Appl. Phys.* **107**, 073517, 1 (2010).
- [27] K. J. Siemsen and H. D. Riccius, *J. Phys. Chem. Solids*, **30**, 1897 (1996).

Received: 27 April, 2013
Accepted: 28 February, 2014